The current issue and full text archive of this journal is available at
www.emeraldinsight.com/0961-5539.htm

A unified fractional step method for compressible and incompressible flows, heat transfer and incompressible solid mechanics

Received 6 December 2005
Revised 2 January 2007
Accepted 2 January 2007

P. Nithiarasu
School of Engineering, University of Wales Swansea, Swansea, UK

Abstract

Purpose – This paper aims to present briefly a unified fractional step method for fluid dynamics, incompressible solid mechanics and heat transfer calculations. The proposed method is demonstrated by solving compressible and incompressible flows, solid mechanics and conjugate heat transfer problems.

Design/methodology/approach – The finite element method is used for the spatial discretization of the equations. The fluid dynamics algorithm used is often referred to as the characteristic-based split scheme.

Findings – The proposed method can be employed as a unified approach to fluid dynamics, heat transfer and solid mechanics problems.

Originality/value – The idea of using a unified approach to fluid dynamics and incompressible solid mechanics problems is proposed. The proposed approach will be valuable in complicated engineering problems such as fluid-structure interaction and problems involving conjugate heat transfer and thermal stresses.

Keywords Fluid dynamics, Solids, Finite element analysis, Meshes

Paper type Research paper

1. Introduction

One of the successful algorithms for incompressible fluid dynamics is the fractional step method (Chorin, 1968). Time and again this method emerged as one of the best procedures for incompressible flow computations, due to its simplicity and effectiveness. Owing to a huge number of papers available on this method, we focus only on the archival and finite element papers. For further, detailed list of papers on this topic, readers are referred to the references cited in the recent works listed at the end. The original fractional step procedure introduced by Chorin has been further studied by many (Kim and Moin, 1985; Comini and Del Guidice, 1982; Kawahara and Ohmiya, 1985; Schneider *et al.*, 1978; Donea *et al.*, 1982; Gresho *et al.*, 1984; Rice and

This paper is partly based on the Keynote Lecture delivered at the 4th International Conference on Heat Transfer, Fluid Mechanics and Thermodynamics (HEFAT2005), Cairo, September 2005.

The author acknowledges the partial financial support received from the Royal Society, UK to attend the HEFAT2005 Conference. The author also thanks the organizers of HEFAT2005, Professor J. Meyer and Dr A.G. Malan, for inviting him to give a keynote lecture.

0961-5539
DOI 10.1108/09615530810846284

Schnipke, 1986; Ramaswamy *et al.*, 1986; Rannacher, 1993; Ren and Utnes, 1993). This method has been combined with other aspects to improve performance and to apply to other fields of interest such as compressible high-speed flows and solid mechanics (Zienkiewicz *et al.*, 2005a, 1999a; Zienkiewicz and Codina, 1995; Nithiarasu, 2003, 2006; Nithiarasu *et al.*, 2004; Nithiarasu and Zienkiewicz, 2006; Bonet and Burton, 1998; Bonet *et al.*, 2001).

The origin of the fractional step method can be traced back to the pioneering work of Chorin (1968) in the finite difference context. Many others generalized the method to finite element discretization (Comini and Del Guidice, 1982; Kawahara and Ohmiya, 1985; Schneider *et al.*, 1978; Donea *et al.*, 1982; Gresho *et al.*, 1984; Rice and Schnipke, 1986; Ramaswamy *et al.*, 1986; Rannacher, 1993; Ren and Utnes, 1993). The accuracy of the method has been the subject of recent research for many (Brown *et al.*, 2001; Chang *et al.*, 2002). Over the last ten years, the fractional step method has been combined with a simple characteristic-based time discretization and extended to unstructured and finite element-based compressible and incompressible flow calculations (Zienkiewicz *et al.*, 2005a; Zienkiewicz and Codina, 1995). The basis of the characteristic-based spit (CBS) scheme and its applications have been discussed in many of the articles published in the past (Zienkiewicz and Codina, 1995; Zienkiewicz *et al.*, 1999b; Nithiarasu, 2005, 2003, 2002; Nithiarasu *et al.*, 2004, 2005; Nithiarasu and Liu, 2005, 2006). Our objective here is, thus, not to review the CBS scheme in detail but to introduce a unified matrix free approach to fluid and solid problems.

The explicit CBS scheme based on an artificial compressibility was introduced in reference (Nithiarasu, 2003). The method was developed by combining a classical fractional step method with an artificial compressibility scheme. The characteristic-based higher order time stepping was adopted to reduce oscillations in convection dominated flows. The pressure stabilization was achieved by introducing fractional stages into the solution process.

The explicit fractional step method can be derived from a semi- or fully discrete form of the Navier-Stokes equations (Nithiarasu and Zienkiewicz, 2006). We employ only the method derived from the semi-discrete form of the equations in this paper. In the past the explicit fractional step method reviewed above was seen mainly as a unified approach to compressible and incompressible flow problems. Though some previous work on solid dynamics was reported (Zienkiewicz *et al.*, 1999a), previously reported method was limited by the purely explicit time stepping restricted by the bulk modulus of the material. In this paper, the method of circumventing such restriction is proposed via a local time stepping approach. In addition to compressible and incompressible flow examples, an example of linear, incompressible elasticity is also presented to demonstrate that the proposed method is a unified approach to both fluid and solid problems.

2. Problem statement

The generalized fluid dynamics equation in conservation form may be written as:

- *Mass conservation:*

$$\frac{\partial \rho}{\partial t} = -\frac{\partial U_i}{\partial x_i} \tag{1}$$

where ρ is the density and t is the time. We define the mass flow flux as:

$$U_i = \rho u_i \tag{2}$$

- *Momentum conservation:*

$$\frac{\partial U_i}{\partial t} = -\frac{\partial}{\partial x_j}(u_j U_i) + \frac{\partial \sigma_{ij}^d}{\partial x_j} - \frac{\partial p}{\partial x_i} + Q_m \tag{3}$$

- *Energy conservation:*

$$\frac{\partial(\rho E)}{\partial t} = -\frac{\partial}{\partial x_i}(u_i \rho E) + \frac{\partial}{\partial x_i}\left(k\frac{\partial T}{\partial x_i}\right) - \frac{\partial}{\partial x_i}(u_i p) + \frac{\partial}{\partial x_i}\left(\sigma_{ij}^d u_j\right) + Q_e \tag{4}$$

where u_i are the velocity components, T is the absolute temperature, Q represents source terms, k is the thermal conductivity, $E = c_v T + (1/2)u_i u_i$, c_v is the specific heat at constant volume and σ_{ij}^d are the deviatoric stress components given by:

$$\sigma_{ij}^d = \mu\left(\frac{\partial u_i}{\partial x_j} + \frac{\partial u_j}{\partial x_i} - \frac{2}{3}\,\delta_{ij}\frac{\partial u_k}{\partial x_k}\right) \tag{5}$$

where δ_{ij} is the Kronecker delta. In general, μ the dynamic viscosity, in the above equation is a function of temperature, $\mu(T)$, and the following relation is used in compressible flow calculations (Hirsch, 1988):

$$\mu = \frac{1.45T^{3/2}}{T + 110} \times 10^{-6} \tag{6}$$

where T is expressed in Kelvins.

The universal gas law or other appropriate constitutive equation is needed when the flow is coupled and compressible. In this paper, following universal gas law is used:

$$p = \rho R T \tag{7}$$

where R is the universal gas constant. In addition, the thermodynamic relation relating pressure and energy is given as:

$$p = (\gamma - 1)\left(\rho E - \frac{1}{2}\frac{U_i U_i}{\rho}\right) \tag{8}$$

The compressible flow problem statement is completed with the following boundary conditions:

$$\phi_i = \bar{\phi}_i \ \text{ on } \ \Gamma_\phi \quad \text{and} \quad q = \bar{q} \ \text{ on } \ \Gamma_f \tag{9}$$

in which:

$$\Gamma = \Gamma_\phi \cup \Gamma_f \tag{10}$$

where ϕ_i indicate the variables and q is the flux (or traction).

With a constant density assumption, the non-conservation form of conservation of mass and momentum may be written for incompressible flows as:

$$\frac{\partial \rho}{\partial t} \approx \frac{1}{\beta^2}\frac{\partial p}{\partial t} = -\rho \frac{\partial u_i}{\partial x_i} \tag{11}$$

where β here is an artificial compressibility, and:

$$\frac{\partial u_i}{\partial t} = -u_j \frac{\partial u_i}{\partial x_j} + \frac{1}{\rho}\frac{\partial \tau_{ij}}{\partial x_j} - \frac{1}{\rho}\frac{\partial p}{\partial x_i} + \frac{Q_m}{\rho} \tag{12}$$

Further, the deviatoric stress relation could be simplified if divergence free velocity field is assumed.

For incompressible flow problems, the simplified form of energy equation may be written as:

$$\rho c_p \left(\frac{\partial T}{\partial t} + u_j \frac{\partial T}{\partial x_j}\right) = \frac{\partial}{\partial x_i}\left(k \frac{\partial T}{\partial x_i}\right) \tag{13}$$

where c_p is the specific heat at constant pressure.

The relationship between the incompressible fluid dynamics equations and solid mechanics equations may be established as follows. The equilibrium equations of an isothermal elastic solid may be written as (without body forces):

$$\frac{\partial \sigma_{ij}}{\partial x_j} = 0 \tag{14}$$

where σ_{ij} is the total stress tensor and may be expressed in terms of deviatoric stress and pressure (volumetric stress) as:

$$\sigma_{ij} = \sigma_{ij}^d - p\delta_{ij} \tag{15}$$

The negative sign of pressure term makes it easy to employ the numerical schemes developed for fluid dynamics problems. Substituting equation (14) into equation (15), we get the following equation:

$$\frac{\partial \sigma_{ij}^d}{\partial x_j} - \frac{\partial p}{\partial x_i} = 0 \tag{16}$$

The above equation is identical to the Stokes flow momentum equation. The constitutive relation for incompressible solid problems may be expressed in terms of displacements as:

$$\sigma_{ij}^d = G\left(\frac{\partial u_i}{\partial x_j} + \frac{\partial u_j}{\partial x_i} - \frac{2}{3}\frac{\partial u_k}{\partial x_k}\delta_{ij}\right) \tag{17}$$

where G is the rigidity modulus. For fluid problems, this is replaced with the dynamic viscosity of the fluid. Since, equation (16) is now written in terms of pressure and displacements, we need an additional equation to close the problem. For incompressible materials the additional equation may be obtained via the incompressibility constraint (volumetric strain), i.e.:

$$\frac{\partial u_i}{\partial x_i} = 0 \tag{18}$$

Equations (16) and (18) may now be solved in a coupled sense to obtain a solution. Many methods for solving the mentioned equation exhibit oscillatory behavior. Also, the discretization of the above equilibrium equations normally results in a set of linear simultaneous equations, which need an efficient solution procedure to handle. To obtain a matrix free formulation, we rewrite the incompressible solid mechanics equations, following fluid dynamics approach, as:

- *Continuity:*

$$\frac{1}{c^2}\frac{\partial p}{\partial t} + \rho\frac{\partial \dot{u}_i}{\partial x_i} = 0 \tag{19}$$

- *Momentum:*

$$\frac{\partial \dot{u}_i}{\partial t} = -\frac{1}{\rho}\frac{\partial p}{\partial x_i} + \frac{1}{\rho}\frac{\partial \sigma_{ij}^d}{\partial x_j} \tag{20}$$

For steady state calculations, the acceleration terms $\dot{u}_i$ in the above equations are replaced with u_i. In the above equations, c (square root of the ratio of the bulk modulus K and density ρ) is the wave speed, which is very large for incompressible materials. If we introduce an artificial, finite c value and iterate using pseudo time t to steady state, we will be able to obtain a static solution to equations (19) and (20). It is also clear that equation (19) will approach the divergence free state (equation (18)) at pseudo steady state and gives the displacement and pressure distribution for an incompressible elastic material.

3. Non-dimensional form

All the results presented in this paper are generated from non-dimensional form of equations. The non-dimensional scales vary depending on the type of problem solved. The following subsections explain various non-dimensional scales used here.

3.1 Compressible flows

The following non-dimensional scales are used for compressible flows:

$$t^* = \frac{tu_\infty}{L};\quad x_i^* = \frac{x_i}{L};\quad \rho^* = \frac{\rho}{\rho_\infty};\quad p^* = \frac{p}{\rho_\infty u_\infty^2}$$
$$u_i^* = \frac{u_i}{u_\infty};\quad E^* = \frac{E}{u_\infty^2};\quad T^* = \frac{Tc_p}{u_\infty^2};\quad c^* = \frac{c}{u_\infty} \tag{21}$$

The non-dimensional form of the equations becomes:

- *Mass conservation:*

$$\frac{\partial \rho^*}{\partial t^*} = -\frac{\partial U_i^*}{\partial x_i^*} \tag{22}$$

- *Momentum conservation:*

$$\frac{\partial U_i^*}{\partial t^*} = -\frac{\partial}{\partial x_j^*}\left(u_j^* U_i^*\right) + \frac{1}{Re}\frac{\partial\left(\nu^* \sigma_{ij}^{d*}\right)}{\partial x_j^*} - \frac{\partial p^*}{\partial x_i^*} \tag{23}$$

- *Energy conservation:*

$$\begin{aligned}\frac{\partial(\rho^* E^*)}{\partial t^*} = & -\frac{\partial}{\partial x_i^*}\left(u_i^* \rho^* E^*\right) + \frac{1}{Re\,Pr}\frac{\partial}{\partial x_i^*}\left(k^* \frac{\partial T^*}{\partial x_i^*}\right) - \frac{\partial}{\partial x_i^*}\left(u_i^* p^*\right) \\ & + \frac{1}{Re}\frac{\partial}{\partial x_i^*}\left(\nu^* \sigma_{ij}^{d*} u_j^*\right)\end{aligned} \tag{24}$$

where Re is the Reynolds number, Pr is the Prandtl number, ν^* is the viscosity ratio and k^* is the conductivity ratio. These parameters are defined as:

$$Re = \frac{u_\infty L}{\nu_\infty}; \quad Pr = \frac{\mu_\infty c_p}{k_\infty}; \quad \nu^* = \frac{\nu}{\nu_\infty}; \quad k^* = \frac{k}{k_\infty} \tag{25}$$

and:

$$\sigma_{ij}^{d*} = \left(\frac{\partial u_i^*}{\partial x_j^*} + \frac{\partial u_j^*}{\partial x_i^*} - \frac{2}{3}\,\delta_{ij}\frac{\partial u_k^*}{\partial x_k^*}\right) \tag{26}$$

In the above equations, subscript ∞ indicates a reference quantity and L is a characteristic dimension.

3.2 Incompressible solid

The non-dimensional scales used here are:

$$u_i^* = \frac{u_i}{L}; \quad t^{2*} = \frac{t^2 G_\infty}{\rho L^2}; \quad x_i^* = \frac{x_i}{L}; \quad p^* = \frac{p}{G_\infty}; \quad K^* = \frac{K}{G_\infty} \tag{27}$$

Substituting the above scales into the equations gives:

- *Continuity:*

$$\frac{1}{K^*}\frac{\partial p^*}{\partial t^*} + \frac{\partial \dot{u}_i^*}{\partial x_i^*} = 0 \tag{28}$$

- *Momentum:*

$$\frac{\partial \dot{u}_i^*}{\partial t^*} = -\frac{\partial p^*}{\partial x_i^*} + G^* \frac{\partial \sigma_{ij}^{d*}}{\partial x_j^*} \tag{29}$$

where $G^* = G/G_\infty$. In the steady state calculation reported in this paper, $\dot{u}_i^*$ is replaced with u_i^* and K^* is replace with c^{*2}.

3.3 Incompressible thermal flow problems

For conjugate heat transfer problems, following scales are suitable:

$$t^* = \frac{t\alpha_\infty}{L^2}; \quad x_i^* = \frac{x_i}{L}; \quad p^* = \frac{pL^2}{\rho_\infty \alpha_\infty^2}$$

$$\beta^* = \frac{\beta L}{\alpha_\infty}; \quad u_i^* = \frac{u_i L}{\alpha_\infty}; \quad T^* = \frac{T - T_\infty}{T - T_w} \tag{30}$$

The non-dimensional form of the governing equations are, continuity:

$$\frac{1}{\beta^{2*}} \frac{\partial p^*}{\partial t^*} = -\frac{\partial u_i^*}{\partial x_i^*}, \tag{31}$$

momentum:

$$\frac{\partial u_i^*}{\partial t^*} = -u_j^* \frac{\partial u_i^*}{\partial x_j^*} + Pr \frac{\partial \sigma_{ij}^{d*}}{\partial x_j^*} - \frac{\partial p^*}{\partial x_i^*} \tag{32}$$

and energy:

$$\frac{\partial T^*}{\partial t^*} + \frac{\partial}{\partial x_j^*} \left(u_j^* T^* \right) = \frac{\partial}{\partial x_i^*} \left(\frac{\alpha}{\alpha_\infty} \frac{\partial T^*}{\partial x_i^*} \right) \tag{33}$$

where $\alpha = k/\rho c_p$ is the thermal diffusivity and $\alpha_\infty = \alpha_{\text{fluid}}$ is assumed in this study.

4. Explicit fractional step method

It is clear from the equations discussed in the previous section that similarity exists between fluid and solid problems. Thus, it will be sufficient to develop a single algorithm to solve these problems. Let us assume the form of compressible flow equations and discretize the density and momentum equations in time as follows:

$$\frac{\Delta \rho}{\Delta t} = \frac{\rho^{n+1} - \rho^n}{\Delta t} = -\frac{\partial U_i^n}{\partial x_i} \tag{34}$$

and:

$$\frac{\Delta U_i}{\Delta t} = \frac{U_i^{n+1} - U_i^n}{\Delta t} = -\frac{\partial}{\partial x_j} \left(u_j U_i \right)^n + \frac{\partial \sigma_{ij}^{dn}}{\partial x_j} - \frac{\partial p^n}{\partial x_i} + Q_m \tag{35}$$

It is well known that the above system will be unconditionally unstable if either appropriate upwinding treatment of convection terms is not employed or if the pressure is not stabilized. There are several convection and pressure stabilized schemes available in the literature but we limit our attention towards achieving stabilization via higher order time stepping and fractional steps. By assuming a CBS stabilization, one can achieve stable and sensible solution.

4.1 Explicit CBS scheme using semi-discrete form

The classic CBS scheme may be derived by assuming individual momentum component equations as convection-diffusion equations and by removing the pressure term from the momentum equations. The time discretization is carried out along the characteristic of the these equations and a Taylor expansion is employed to treat the semi-discrete equations at the same spatial position (Zienkiewicz and Codina, 1995; Zienkiewicz *et al.*, 1999b; Nithiarasu, 2005). With such an expansion, the first step of the CBS scheme in its semi-discrete form may be written as:

(1) *Step 1. Intermediate momentum:*

$$\begin{aligned}\Delta U_i^* &= U_i^* - U_i^n \\ &= \Delta t\left[-\frac{\partial}{\partial x_j}(U_i u_j) + \frac{\partial \sigma_{ij}^d}{\partial x_j} - \rho g_i\right]^n \\ &\quad + \frac{\Delta t^2}{2} u_k \frac{\partial}{\partial x_k}\left(\frac{\partial}{\partial x_j}(U_i u_j) + \frac{\partial p}{\partial x_i} - \frac{\partial \sigma_{ij}^d}{\partial x_j} + \rho g_i\right)^n\end{aligned} \tag{36}$$

where $U_i^n = U_i(t_n); \Delta t = t^{n+1} - t^n$ and * indicates an intermediate quantity. In the above equation, the last term is a result of the Taylor expansion and this second order extra term acts as a convection stabilization operator. The above intermediate stage needs a correction step, which is the third step of the CBS scheme (equation (38)). Substituting the correction step into the conservation of mass equation (34), and reorganizing we get:

(2) *Step 2. Pressure:*

$$\begin{aligned}\Delta\rho &= (\rho^{n+1} - \rho^n) \\ &= -\Delta t\left[\frac{\partial U_i^n}{\partial x_i} + \theta_1 \frac{\partial \Delta U_i^*}{\partial x_i} - \Delta t \theta_1\left(\frac{\partial^2 p^n}{\partial x_i \partial x_i} + \theta_2 \frac{\partial^2 \Delta p}{\partial x_i \partial x_i}\right)\right]\end{aligned} \tag{37}$$

As seen two parameters, θ_1 and θ_2, are introduced in the above equation. θ_1 is a stabilization parameter, which is introduced by treating the right hand side of equation (34) at $n + \theta_1$ level. The stabilization parameter θ_1 must be above zero to get any pressure stability. The parameter θ_2 is introduced to move between explicit and implicit treatment of the RHS pressure term. In this paper, we adopt $\theta_2 = 0$, which means that the RHS pressure terms are treated explicitly at Step 2.

Once the relation between the pressure and intermediate momentum is established, we can return to the correction stage, where the actual velocity is computed at the third step as shown below.

(3) *Step 3. Momentum correction:*

$$\Delta U_i = U_i^{n+1} - U_i^n = \Delta U_i^* - \Delta t \frac{\partial p^n}{\partial x_i} \tag{38}$$

Once the above three steps are completed, the energy calculation is carried out as the fourth step.

(4) *Step 4. Energy calculation:*

$$\frac{(\rho E)^{n+1}-(\rho E)^n}{\Delta t}=-\frac{\partial}{\partial x_i}(u_i\rho E)^n+\frac{\partial}{\partial x_i}\left(k\frac{\partial T}{\partial x_i}\right)^n-\frac{\partial}{\partial x_i}(u_ip)^n+\frac{\partial}{\partial x_i}\left(\sigma_{ij}^d u_j\right)^n$$

$$+Q_e^n+\frac{\Delta t}{2}u_k\frac{\partial}{\partial k}\left(\frac{\partial}{\partial x_i}(u_i\rho E)^n-\frac{\partial}{\partial x_i}\left(k\frac{\partial T}{\partial x_i}\right)^n\right. \qquad (39)$$

$$\left.+\frac{\partial}{\partial x_i}(u_ip)^n-\frac{\partial}{\partial x_i}\left(\sigma_{ij}^d u_j\right)^n-Q_e^n\right)$$

The standard Galerkin approximation can now be applied to all the three steps. Assuming linear variation for all variables, the fully discrete matrix form for the four steps may be written as:

Step 1:

$$\mathbf{M}\Delta\mathbf{U}^*=-\Delta t\mathbf{C}\mathbf{U}^n+\Delta t\mathbf{K}\mathbf{U}^n+\mathbf{K}_s\mathbf{U}^n+\mathbf{F}^n \qquad (40)$$

Assuming $\theta_2=0$.

Step 2:

$$\mathbf{M}\Delta\rho=-\theta_1\Delta t\mathbf{D}\mathbf{U}^n-\theta_1\Delta t\mathbf{D}\Delta\mathbf{U}^*+\theta_1\Delta t\mathbf{L}p^n \qquad (41)$$

The matrix form of the correction step is

Step 3:

$$\mathbf{M}\Delta\mathbf{U}=\tilde{\mathbf{M}}\Delta\mathbf{U}^*-\Delta t\mathbf{G}p^n \qquad (42)$$

and finally the energy equation in its matrix form is

Step 4:

$$\mathbf{M}\Delta\tilde{E}=-\Delta t\left[\mathrm{C}\tilde{E}+\mathrm{C}\tilde{p}+\mathrm{L}\tilde{T}+\mathbf{K}_e\tilde{u}+\frac{\Delta t}{2}\mathbf{K}_s\tilde{E}+\frac{\Delta t}{2}\mathbf{K}_s\tilde{p}+\mathbf{F}_e\right] \qquad (43)$$

In the above equations **C**, **G**, **D**, **L** and **K** are discrete convection, gradient, divergence, Laplacian and viscous operators, $\mathbf{K}_s$ is the stabilization matrix, $\mathbf{K}_e$ is the matrix associated with the work done by deviatoric stresses in the energy equation, **F** and $\mathbf{F}_e$ are the forcing vectors and **M** is the mass matrix. To obtain a matrix free formulation, we lump the mass matrix by summing up the rows for linear elements. In the above equations, $\sim$ represents a nodal vector and $\tilde{E}$ contains the nodal values of ρE. It should be noted that the third and higher order terms are neglected in this study. For further details on the construction of the finite element matrices, the readers are referred to (Zienkiewicz *et al.*, 2005a).

At the discrete stage of the formulation, the Dirichlet conditions for velocity are applied only at Step 3. However, traction conditions can either be applied at Step 1 or at Step 3 (Nithiarasu, 2002).

The equations of incompressible flows and incompressible solids can be discretized in a similar fashion to that of compressible flows detailed above.

5. Different cases

5.1 Compressible flows

In addition to the higher order terms introduced by the characteristic Galerkin discretization, an additional artificial dissipation (Nithiarasu *et al.*, 1998) and/or variable smoothing (Thomas and Nithiarasu, 2005) may also be necessary to get a smooth compressible flow solution. The solution algorithm for compressible flow problems may be summarised as:

(1) Calculate the intermediate momentum.

(2) Calculate density.

(3) Calculate energy.

(4) Calculate pressure (thermodynamic relation).

(5) Calculate local speed of sound and Mach number (gas law).

The transient solution to a compressible flow problem may be obtained via explicit time stepping or via matrix free dual time stepping.

5.2 Solid mechanics

For isothermal incompressible solid problems, the energy equation can be decoupled from other equations. The speed of sound c is replaced with a pseudo value β calculated as (Nithiarasu, 2006):

$$\beta = \max(v_1, v_2) \tag{44}$$

where v_1 and v_2 are the wave speeds due to the rigidity modulus and local change in displacements, respectively. These values are defined as:

$$v_1 = \frac{G^\dagger \tau^*}{h}; v_2 = \sqrt{u_i u_i} \tag{45}$$

Here, $G^\dagger = (G/\rho)$, τ^* is a time scale and h is the local element size. The time scale τ^* is taken equal to 2.0 based on the observations in fluid dynamics calculations (Malan *et al.*, 2002; Nithiarasu, 2003). The local nodal element size for linear triangles is calculated as the minimum size of the elements surrounding a node (Zienkiewicz *et al.*, 2005a).

To obtain a solution for an incompressible elastic solid problem, equations (19) and (20) are solved using the fractional steps to steady state. However, a transient algorithm can be developed using the following dual time stepping approach if necessary. We introduce a discrete approximation to the true transient term, $\partial^2 u_i / \partial \tau^2$, to the RHS of the correction step (Nithiarasu, 2006) (assuming viscous resistance equal to zero):

$$u_i^{n+1} = \tilde{u}_i - \frac{1}{\rho} \Delta t \frac{\partial p^n}{\partial x_i} - \Delta t \frac{u_i^{m+1} - 2u_i^m + u_i^{m-1}}{\Delta \tau^2} \tag{46}$$

where superscripts $m+1$, m and $m-1$ represent the real time variation. At pseudo steady state $u_i^{n+1} = u_i^n = u_i^{m+1}$. This immediately shows that the pseudo time stepping is simply used as an iterative mechanism to obtain a transient solution. During each real time step $u_i^{n+1} \approx u_i^n$ and $p^{n+1} \approx p^n$ need to be maintained to get an accurate transient solution.

5.3 Incompressible thermal flow

Here, a pseudo compressibility factor β is introduced in place of c again to decouple the energy equation from other equations (Nithiarasu, 2003). The artificial compressibility factor is calculated as:

$$\beta = \max\left(\varepsilon, \sqrt{u_i u_i}, \frac{2\nu}{h}, \frac{2\alpha}{h}\right) \tag{47}$$

where ε is a small real number. The optimal value (from experience) of this quantity is 0.5. A dual time stepping procedure similar to the solid mechanics discussed above is essential to get transient state (Nithiarasu, 2003).

6. Numerical examples

The numerical examples are considered under three different categories. Only sample problems are given here and for further details the readers are referred to other papers by the author in this area.

6.1 Compressible flow

Here, inviscid flow past an NACA0012 aerofoil is considered in two dimensions. Figure 1 shows the domain used and the unstructured mesh. As seen the mesh is very fine close to the aerofoil surface. The inlet Mach number for the problem is at a subsonic speed of 0.85. The angle of attack at inlet is 0° to the horizontal. The domain consists of inlet, exit and wall boundaries. At inlet the free stream velocity is prescribed and at exit density is prescribed. The energy value at inlet is calculated from the free stream velocity and Mach number and forced. The calculation starts with initial conditions of $\rho^* = 1, u_1^* = 1$ and $u_2^* = 0$.

Figures 2 and 3 show the result obtained at an inlet Mach number of 0.85. The pressure contours shown in Figure 2 shows the shock on the top surface of the aerofoil. The comparison of the pressure coefficient with the AGARD (Pulliam and Barton, 1985) results show a good agreement with the present result. The fine mesh used is shown in Figure 1. The number of elements used here is 21,000. The coarse mesh consists of about one third of the number of elements in the fine mesh.

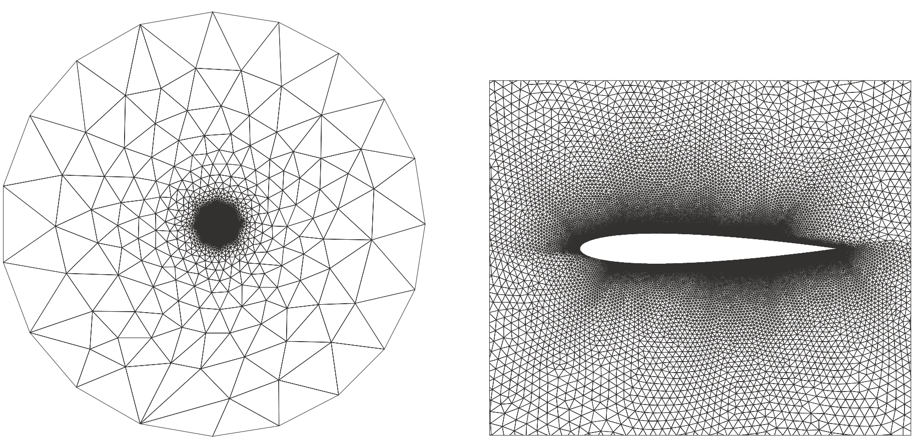

(a) Full domain

(b) Mesh close to the aerofoil

Figure 1. Inviscid flow past a NACA0012 aerofoil. Unstructured mesh

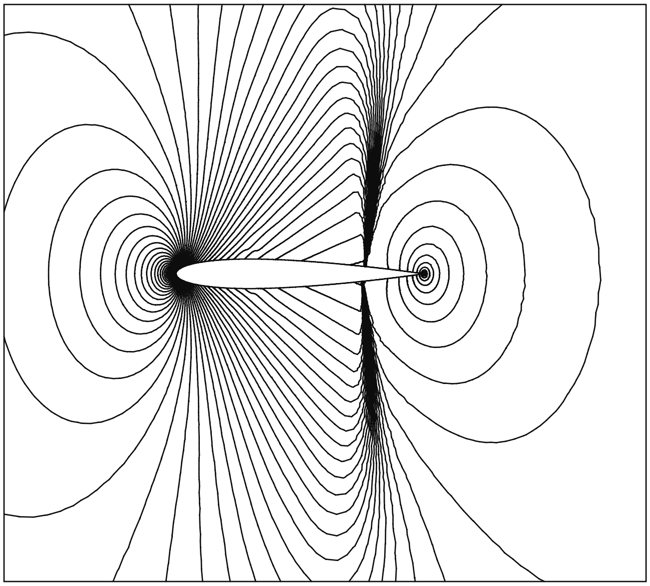

Figure 2.
Inviscid flow past a NACA0012 aerofoil. Contours of pressure

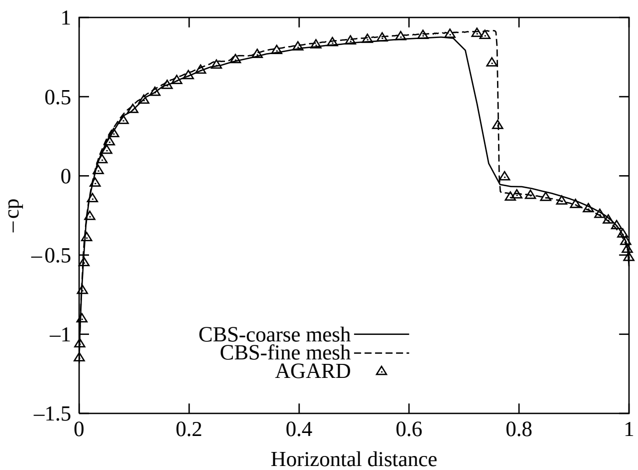

Figure 3.
Inviscid flow past a NACA0012 aerofoil. Pressure coefficient distribution

6.2 Solid mechanics

Here, a square plate with a slot at the centre as shown in Figure 4 is considered. The slot is subjected to zero traction but the top and bottom sides of the plate are subjected to a vertical traction of:

$$t_2 = \tau_{22} - p = 1 \tag{48}$$

The vertical sides are restrained from moving in the horizontal direction but allowed to move in the vertical direction and a G^* value of 8 is used here. The problem has been solved with and without extra pressure stabilization. The extra pressure stabilization was introduced using lumped and consistent mass matrices (Lahiri *et al.*, 2005; Nithiarasu, 2006).

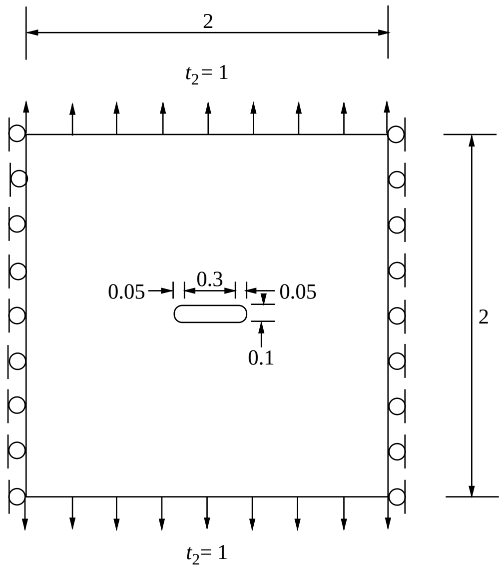

Figure 4.
A slotted tension strip.
Geometry and boundary conditions

To carry out the analysis only one quarter of the domain was used. The mesh used consists of 938 linear triangular elements and 538 nodes. Figure 5 shows the pressure distribution along the axes and vertical displacement along the top horizontal side. The results are also compared against the GLS results (Zienkiewicz *et al.*, 2005b). As seen the agreement of the pressure is generally good among the methods. The extra pressure stabilization eliminated the small pressure oscillation close to the top side. However, the agreement between the extra stabilized results and others are not good for the vertical displacement distribution.

6.3 Incompressible thermal flow

To demonstrate the incompressible fluid dynamics and conjugate heat transfer, forced convection flow and heat transfer in a model fin and tube heat exchanger are studied here. Owing to the low-memory needs and easy implementation, the fully explicit forms is chosen here. The comparison of speed between the fully explicit method with local time stepping against other implicit methods, show that the explicit method is robust and in some cases outperforms the other methods (Codina *et al.*, 2006; Massarotti *et al.*, 2006).

Figure 6 shows a partial representation of the model. The fins are attached to the solid wall of the heat exchanger as shown in the figure. The outside solid surface is assumed to be at a higher temperature than the air flow at the inlet to the heat exchanger. Thus, the heat is expected to pass through the solid wall and then dissipated to the fluid via the inside solid wall surface and the fin surfaces. The fluid side, bottom and top boundaries are subjected to zero flux boundary conditions. The inlet velocity was assumed to be constant and uniform. To demonstrate the method, a inlet Reynolds number of 200 and thermal conductivity ratio between the solid and fluid of 10 are assumed.

Figure 7 shows the unstructured surface mesh used in the calculations. The mesh generated using the meshing tools available within Swansea, School of Engineering

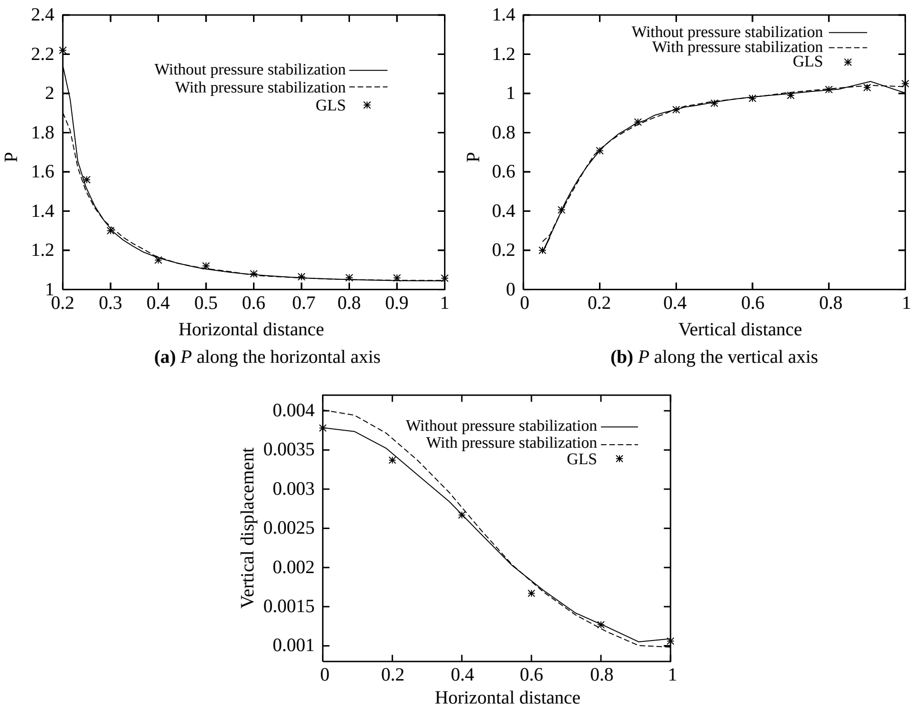

(a) *P* along the horizontal axis

(b) *P* along the vertical axis

(c) Vertical displacement along the top side

Figure 5.
A slotted tension strip. Pressure and displacement distributions

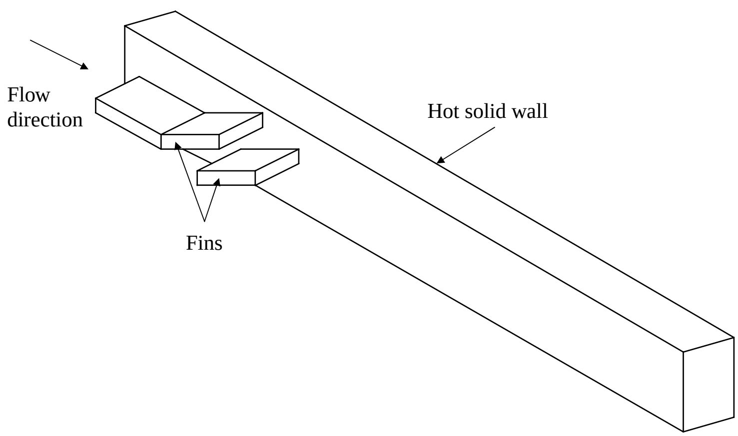

Figure 6.
Conjugate heat transfer in a model fin and tube heat exchanger. Part of the geometry

(Morgan *et al.*, 1999; Weatherill *et al.*, 2001). As seen the mesh is refined close to the solid fluid interface to have smooth change in the temperature distribution. The total number of tetrahedron elements used is just over 1.7 million.

Figures 8-10 show the results obtained. In Figure 8, the surface contours of pressure velocity components and temperature are presented. As seen the contours are generally

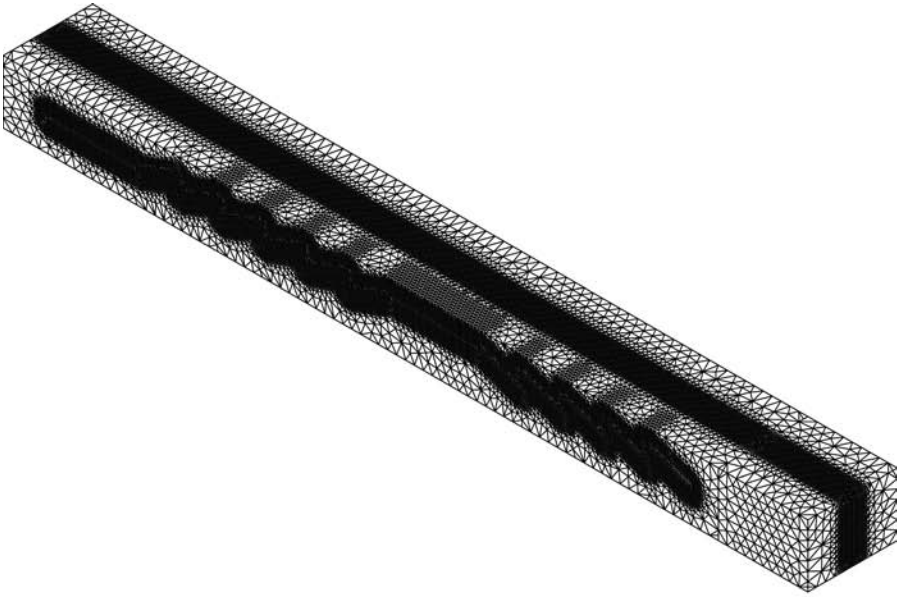

(a) Full view

(b) Fins and surface of the solid wall

Figure 7.
Conjugate heat transfer in a model fin and tube heat exchanger. Unstructured mesh

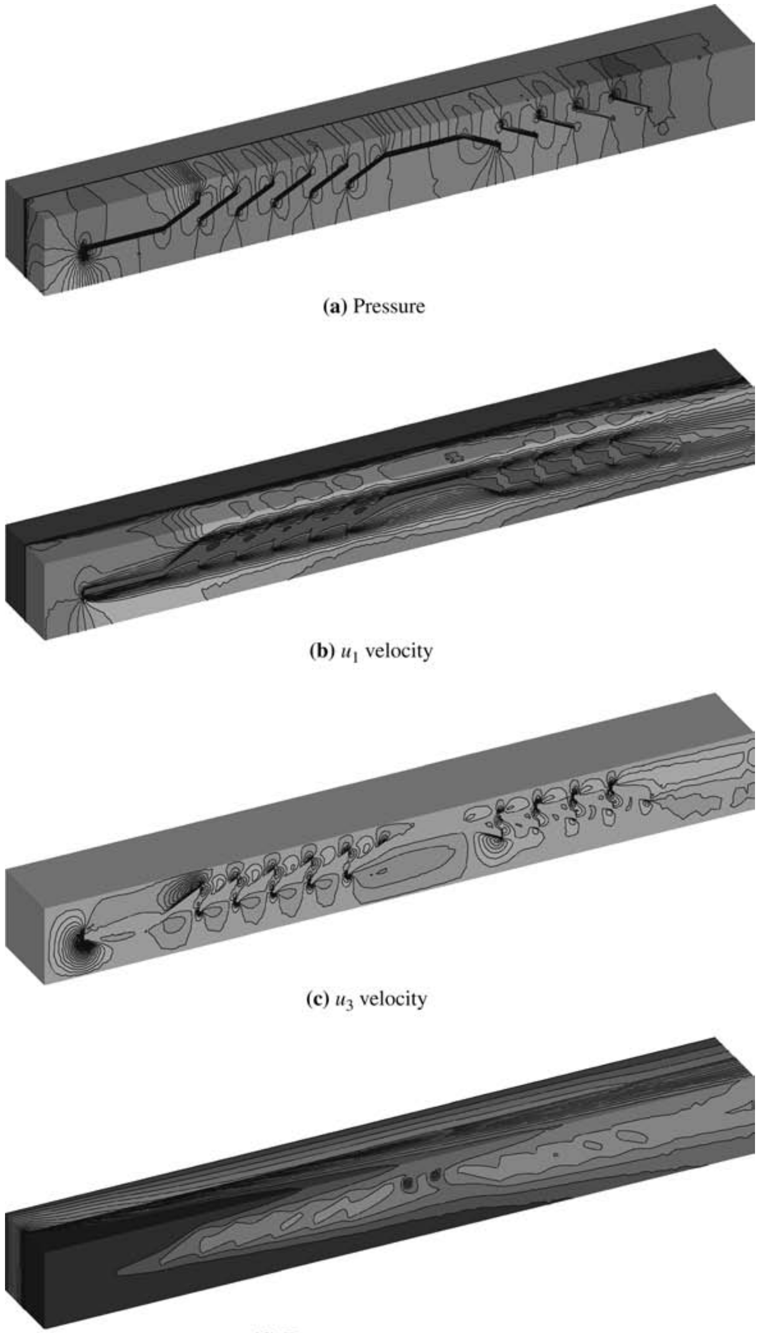

(a) Pressure

(b) u_1 velocity

(c) u_3 velocity

(d) Temperature contours

Figure 8.
Conjugate heat transfer in a model fin and tube heat exchanger. Pressure, velocity and temperature contours

smooth including the pressure solution. In Figure 9, the temperature distribution at different sections, along the length (x_1 direction) of the heat exchanger is presented. As seen the transition of the temperature from solid to fluid is smooth without any noticeable discontinuity.

Figure 10 shows the temperature distribution at sections $x_1 = 2$ and $x_1 = 14$, along different lines. Figure 10(a) shows the temperature distribution in the x_2 direction along the lines at the middle of the fins and Figure 10(b) shows the temperature distribution at $x_2 = 0.523$ along the x_3 direction. Figure 10 (c) and (d) show the temperature distributions along x_2 direction, at sections $x_3 = 0.407$ and 1.064, respectively. As seen

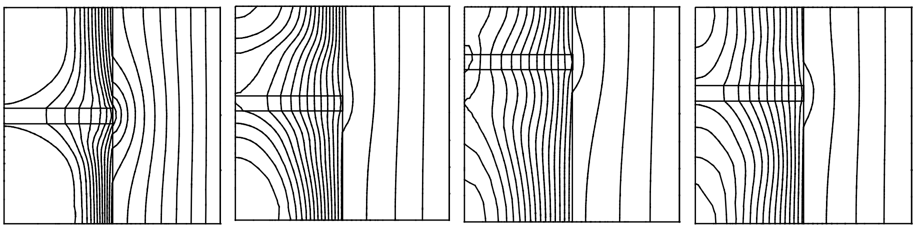

(a) $x_1 = 2$ **(b)** $x_1 = 6$ **(c)** $x_1 = 10$ **(d)** $x_1 = 14$

Figure 9.
Conjugate heat transfer in a model fin and tube heat exchanger. Temperature contours at different sections

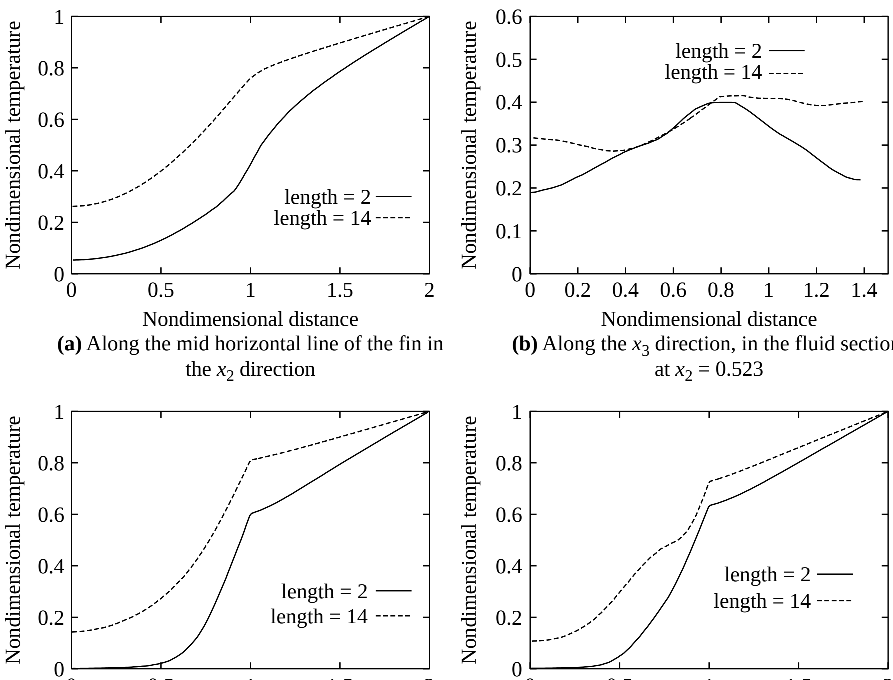

(a) Along the mid horizontal line of the fin in the x_2 direction

(b) Along the x_3 direction, in the fluid section, at $x_2 = 0.523$

(c) Along $x_3 = 0.407$ below the fin in the x_2 direction

(d) Along $x_3 = 1.064$ above the fin in the x_2 direction

Figure 10.
Conjugate heat transfer in a model fin and tube heat exchanger. Temperature distributions

majority of the solid wall portions show a linear variation in temperature. In the fluid region, including fins, the temperature variation is nonlinear. It is also noticed that the no heat flux conditions at the fluid side boundary is effectively captured. In Figure 10 (c) and (d), a rapid change in temperature clearly shows in interface. In addition, the average temperature at section $x_1 = 2$ is much lower than at section $x_1 = 14$ as expected. All the results shown in Figure 10 are consistent with the qualitative solution expected.

7. Conclusions

A unified approach for fluid dynamics and incompressible solid mechanics has been presented. The examples presented demonstrated that a single algorithm can be employed in the calculations of high speed gas flows, low-speed incompressible flows and incompressible solid mechanics. The next obvious step would be to extend the work to more general solid mechanics framework such as generalized elastic and viscoelastic behavior. The proposed approach also provides a platform for carrying out fluid-structure interaction studies using a unified approach.

References

Bonet, J. and Burton, A.J. (1998), "A simple averaged nodal pressure tetrahedral element for nearly incompressible dynamic explicit applications", *Communications in Numerical Methods in Engineering*, Vol. 14, pp. 437-49.

Bonet, J., Marriott, H. and Hassan, O. (2001), "Stability and comparison of different linear tetrahedral formulations for nearly incompressible explicit dynamic applications", *International Journal for Numerical Methods in Engineering*, Vol. 50, pp. 119-33.

Brown, D.L., Cortez, R. and Minion, M.L. (2001), "Accurate projection methods for the incompressible Navier-Stokes equations", *Journal of Computational Physics*, Vol. 168, pp. 464-99.

Chang, W., Giraldo, F. and Perot, B. (2002), "Analysis of an exact fractional step method", *Journal of Computational Physics*, Vol. 180, pp. 183-99.

Chorin, A.J. (1968), "Numerical solution of the Navier-Stokes equations", *Mathematics of Computation*, Vol. 22, pp. 745-62.

Codina, R., Owen, H.C., Nithiarasu, P. and Liu, C.B. (2006), "Numerical comparison of CBS and SGS as stabilization techniques for the incompressible Navier-Stokes equations", *International Journal of Numerical Methods in Engineering*, Vol. 66, pp. 1672-89.

Comini, G. and Del Guidice, S. (1982), "Finite element solution of incompressible Navier-Stokes equations", *Num. Heat Transfer, Part A Applications*, Vol. 5, pp. 463-78.

Donea, J., Giuliani, S., Laval, H. and Quartapelle, L. (1982), "Finite element solution of unsteady Navier-Stokes equations by a fractional step method", *Computer Methods in Applied Mechanics and Engineering*, Vol. 33, pp. 53-73.

Gresho, P.M., Chan, S.T., Lee, R.L. and Upson, C.D. (1984), "A modified finite element method for solving incompressible Navier-Stokes equations. Part I theory", *International Journal for Numerical Methods in Engineering*, Vol. 4, pp. 557-98.

Hirsch, C. (1988), *Numerical Computation of Internal and External Flows, Fundamentals of Numerical Discretization*, Vol. 1, Wiley, New York, NY.

Kawahara, M. and Ohmiya, K. (1985), "Finite element analysis o f density flow using the velocity correction procedure", *International Journal for Numerical Methods in Engineering*, Vol. 5, pp. 981-93.

Kim, J. and Moin, P. (1985), "Application of a fractional step method to incompressible Navier-Stokes equations", *Journal of Computational Physics*, Vol. 59, pp. 308-23.

Lahiri, S.K., Bonet, J., Peraire, J. and Casals, L. (2005), "A variationally consistent fractional time-step integration method for incompressible and nearly incompressible Lagrangian dynamics", *International Journal for Numerical Methods in Engineering*, Vol. 63, pp. 1371-95.

Malan, A.G., Lewis, R.W. and Nithiarasu, P. (2002), "An improved unsteady, unstructured, artificial compressibility, finite volume scheme for viscous incompressible flows: Part I. Theory and implementation", *International Journal for Numerical Methods in Engineering*, Vol. 54, pp. 695-714.

Massarotti, N., Arpino, F., Lewis, R.W. and Nithiarasu, P. (2006), "Explicit and semi-implicit CBS procedures for incompressible viscous flows", *International Journal of Numerical Methods in Engineering*, Vol. 66, pp. 1618-40.

Morgan, K., Weatherill, N.P., Hassan, O., Brookes, P.J., Said, R. and Jones, J. (1999), "A parallel framework for multidisciplinary aerospace engineering simulations using unstructured meshes", *International Journal for Numerical Methods in Fluids*, Vol. 31, pp. 159-73.

Nithiarasu, P. (2002), "On boundary conditions of the CBS algorithm for computational fluid dynamics", *International Journal of Numerical Methods in Engineering*, Vol. 54, pp. 523-36.

Nithiarasu, P. (2003), "An efficient artificial compressibility (AC) scheme based on the characteristic based split (CBS) method for incompressible flows", *International Journal for Numerical Methods in Engineering*, Vol. 56, pp. 1815-45.

Nithiarasu, P. (2005), "An arbitrary Eulerian Lagrangian (ALE) method for free surface flow calculations using the characteristic based split (CBS) scheme", *International Journal for Numerical Methods in Fluids*, Vol. 48, pp. 1415-28.

Nithiarasu, P. (2006), "A matrix free fractional step method for static and dynamic incompressible solid mechanics", *International Journal for Computational Methods in Engineering Science and Mechanics*, Vol. 7 No. 5, pp. 369-80.

Nithiarasu, P. and Liu, C-B. (2005), "Steady and unstable flow calculations in a double driven cavity using the explicit CBS scheme", *International Journal for Numerical Methods in Engineering*, Vol. 63, pp. 380-97.

Nithiarasu, P. and Liu, C-B. (2006), "An explicit characteristic based split (CBS) scheme for incompressible turbulent flows", *Computer Methods in Applied Mechanics and Engineering*, Vol. 7, pp. 369-80.

Nithiarasu, P. and Zienkiewicz, O.C. (2006), "Analysis of an explicit and matrix free fractional step method for incompressible flows", *Computer Methods in Applied Mechanics and Engineering*, Vol. 195, pp. 5537-51.

Nithiarasu, P., Massarotti, N. and Mathur, J.S. (2005), "Forced convection heat transfer from solder balls on a printed circuit board using the characteristic based split (CBS) scheme", *International Journal of Numerical Methods in Heat & Fluid Flow*, Vol. 15, pp. 73-95.

Nithiarasu, P., Mathur, J.S., Weatherill, N.P. and Morgan, K. (2004), "Three-dimensional incompressible flow calculations using the characteristic based split (CBS) scheme", *International Journal for Numerical Methods in Fluids*, Vol. 44, pp. 1207-29.

Nithiarasu, P., Zienkiewicz, O.C., Sai, B.V.K.S., Morgan, K., Codina, R. and Vázquez, M. (1998), "Shock capturing viscosities for the general fluid mechanics algorithm", *International Journal for Numerical Methods in Fluids*, Vol. 28, pp. 1325-53.

Pulliam, T.H. and Barton, J.T. (1985) AIAA 23rd Aerospace Sciences Meeting – Euler computations of AGARD working group 07 airfoil test cases, AIAA Paper – 85-0018.

Ramaswamy, B., Kawahara, M. and Nakayama, T. (1986), "Lagrangian finite element method for the analysis of two dimensional sloshing problems", *International Journal for Numerical Methods in Fluids*, Vol. 6, pp. 659-70.

Rannacher, R. (1993), "On Chorin projection method for the incompressible Navier-Stokes equations", *Lecture Notes in Mathematics*, Vol. 1530, pp. 167-83.

Ren, G. and Utnes, T. (1993), "A finite element solution of the time dependent incompressible Navier-Stokes equations using a modified velocity correction method", *International Journal for Numerical Methods in Fluids*, Vol. 17, pp. 349-64.

Rice, J.G. and Schnipke, R.J. (1986), "An equal-order velocity-pressure formulation that does not exhibit spurious pressure modes", *Computer Methods in Applied Mechanics and Engineering*, Vol. 58, pp. 135-49.

Schneider, G.E., Raithby, G.D. and Yovanovich, M.M. (1978), "Finite element analysis of incompressible flow incorporating equal order pressure and velocity interpolation", in Taylor, C., Morgan, K. and Brebbia, C.A. (Eds), *Numerical Methods in Laminar and Turbulent Flow*, Pentech Press, Plymouth.

Thomas, C. and Nithiarasu, P. (2005), "Influences of element size and variable smoothing on inviscid compressible flow solution", *International Journal of Numerical Methods for Heat and Fluid Flow*, Vol. 15, pp. 420-8.

Weatherill, N.P., Hassan, O., Morgan, K., Jones, J.W. and Larwood, B. (2001), "Towards fully parallel aerospace simulations on unstructured meshes", *Engineering Computations*, Vol. 18, pp. 347-75.

Zienkiewicz, O.C. and Codina, R. (1995), "A general algorithm for compressible and incompressible flow – Part I: the split, characteristic-based scheme", *International Journal for Numerical Methods in Fluids*, Vol. 20, pp. 869-85.

Zienkiewicz, O.C., Taylor, R.L. and Nithiarasu, P. (2005a), *The Finite Element Method for Fluid Dynamics*, 6th ed., Elsevier, Amsterdam.

Zienkiewicz, O.C., Taylor, R.L. and Zhu, J.Z. (2005b), *The Finite Element Method. Its Basis & Fundamentals*, 6th ed., Elsevier, Amsterdam.

Zienkiewicz, O.C., Rojek, J., Taylor, R.L. and Pastor, M. (1999a), "Triangles and tetrahedra in explicit dynamic codes for solids", *International Journal for Numerical Methods in Engineering*, Vol. 43, pp. 565-83.

Zienkiewicz, O.C., Nithiarasu, P., Codina, R., Vázquez, M. and Ortiz, P. (1999b), "The characteristic based split procedure: an efficient and accurate algorithm for fluid problems", *International Journal for Numerical Methods in Fluids*, Vol. 31, pp. 359-92.

Further reading

Gresho, P.M. and Sani, R.L. (2000), *Incompressible Floe and the Finite Element Method, Isothermal Laminar Flow*, Vol. 2, Wiley, New York, NY.

Shuen, J.S., Chen, K.H. and Choi, Y.H. (1993), "A coupled implicit method for chemical non-equilibrium flows at all speeds", *Journal of Computational Physics*, Vol. 106, pp. 306-18.

Corresponding author

P. Nithiarasu can be contacted at: P.Nithiarasu@swansea.ac.uk